Physics – Uspekhi **61** (10) 952 – 964 (2018)

REVIEWS OF TOPICAL PROBLEMS PACS numbers: 03.65.Nk, 03.75.Be, **41.85.–p**, 42.25.Fx, **78.70.–g**

Goos–Hänchen effect in neutron optics and the reflection time of neutron waves

V A Bushuev, A I Frank

DOI: https://doi.org/10.3367/UFNe.2017.11.038235

Contents

Abstract. The Goos – Hänchen (GH) effect, a longitudinal shift of a wave beam at total internal reflection, is well known in optics and has been repeatedly observed for light, micro-, and ultrasonic waves. We consider the GH effect for a massive particle reflected from a material boundary. A close relation is shown to exist between the longitudinal shift and the time delay of reflection. In the case of a neutron reflected from a planar resonant system, a giant longitudinal shift of either positive or negative sign can occur, corresponding to a large reflection group delay time. This time can also be negative, which does not contradict the causality principle. Prospects of the experimental observation of the GH effect and group delay time for neutron reflection are reviewed.

Keywords: neutron optics, wave beams, Goos – Hänchen effect, group delay time, reflection from multilayer structures

1. Introduction

The discovery of a longitudinal shift of a wave packet in the case of total internal reflection in the optical wavelength range, which was named the Goos–Hänchen (GH) effect [1, 2], strongly influenced the development of concepts in reflection physics. Such an apparent violation of geometric optics laws induced a series of theoretical [3–20] and experimental [21–27] studies that continue to date. It became clear very early that this phenomenon has a very general nature, and studying the phenomenon went beyond usual optics. The GH shift was observed for acoustic waves [5, 28–31] and, later, for microwave radiation [32–36] and X-rays [37].

The longitudinal shift was found to be one in a series of reflection-related effects. A transverse shift of reflected electromagnetic waves was predicted in [38] and then discovered experimentally in [39, 40]. Later, the GH transverse shift and the Fedorov–Imbert sideways shift [38, 39] started being viewed as two manifestations of the same wave phenomenon [41–45]. It was also found that wave beams exhibit a shift along the propagation direction, the so-called focal shift, with the wave beam reflection angle not exactly equal to the incidence angle, thus defying Snell's law [11, 36, 46, 47].

The existence of the GH shift for a massive particle reflected from a region with a potential seems then to be quite obvious. An analysis of the underlying quantum problem seems to have been first conducted in [48] and has afterwards been repeated many times [6, 49]. The quantum mechanical approach proved to be especially effective after a direct relation between the GH effect and the quantum problem of the reflection time [50] had been understood.

Although the history of the problem extends over more than fifty years, the GH shift for a reflected massive particle has so far remained in the realm of theory. The best conditions for experimental observation of the phenomenon seem to be offered by neutron optics. To the best of our knowledge, Seregin was the first to consider the GH effect for bounced neutrons [51]. Later, the theory of the phenomenon and options for observing the effect in neutron experiments were discussed in [52, 53]. Paper [54], which reported an observation of the GH effect in neutron optics, led to a discussion [55, 56], thus making the problem even more relevant [57].

V A Bushuev Lomonosov Moscow State University, Faculty of Physics, Leninskie gory 1, str. 2, 119991 Moscow, Russian Federation
E-mail: vabushuev@yandex.ru
A I Frank Joint Institute for Nuclear Research, Frank Laboratory of Neutron Physics, ul. Joliot Curie 6, 141980 Dubna, Moscow region, Russian Federation
E-mail: frank@nf.jinr.ru

Received 14 April 2017, revised 6 November 2017
Uspekhi Fizicheskikh Nauk **188** (10) 1049 – 1062 (2018)
DOI: https://doi.org/10.3367/UFNr.2017.11.038235
Translated by M Zh Shmatikov; edited by A M Semikhatov

We here consider some aspects of the GH effect for a massive particle. Section 2 contains background information about the nature of the GH effect. A formal relation between the Artmann formula [3] for the longitudinal GH shift and the group delay time for a bounced massive particle is emphasized. We also compare two approaches (see [3, 6]) to the theory of the GH effect, the results of which have long been considered incompatible.

In Section 3, the reflection of neutron waves from multilayer structures is considered. A calculation of the group delay time for waves reflected from such structures, which is done within a plane-wave approximation, is presented. Resonant enhancement of the longitudinal shift is shown to occur in the case of reflection on multilayer structures. It is noteworthy that the giant shift and delay time can be both positive and negative.

Section 4 contains a more accurate theory of the reflection of collimated neutron beams and wave packets limited in time. It is shown that a wave packet reflected from a resonant structure can actually have a negative 'delay' time; however, this phenomenon is related to changes in the packet shape and does not contradict the causality principle.

In Section 5, the prospects of experimental observation of the longitudinal shift of a neutron beam and the time of its reflection from multilayer structures are discussed.

2. Goos–Hänchen shift and the time of neutron reflection from matter. The plane-wave approximation

A specific feature of neutron optics is that in the majority of cases the neutron wave interaction with matter can be described by introducing the effective potential

$$U = \frac{2\pi\hbar^2}{m}\,\rho b\,, \tag{1}$$

where m is the mass of the neutron, ρ is the volume density of atoms, and b is the mean coherent scattering length on atomic nuclei, which is usually positive.

Representing the medium as a constant potential enables considering the motion of a neutron wave along each coordinate axis separately. As a result, the wave vector component normal to the medium boundary is independent of the longitudinal component.

To illustrate in the simplest way how the longitudinal shift of the neutron beam occurs when a neutron wave is reflected from the boundary of a region where the potential is nonzero, we consider a simplified form of Artmann's theoretical approach [3]. The well-known Artmann method was used, with some modifications, in a number of later studies (see, e.g., [4, 5, 20, 52]).

We consider a region of space with some potential U, limited by the plane $z = 0$. We explore the reflection of a wave beam from the boundary and for simplicity, following [18], assume that the beam is formed by only two waves whose wave vectors are oriented in slightly different directions. For each wave, the condition of total external reflection (TER) $E_\mathrm{n} < U$ holds, where

$$E_\mathrm{n} = \frac{\hbar^2 k_z^2}{2m} \tag{2}$$

and k_z is the wave vector component normal to the surface. The medium refractive index for neutrons is $n = (1 - U/E_\mathrm{n})^{1/2}$. In the case under consideration, $b > 0$ and, if $E_\mathrm{n} > U$, the refractive index is less than unity, similarly to the X-ray case. It is for this reason that the total external reflection occurs for neutrons incident on the boundary in the direction from a less dense medium to a denser medium, in contrast to total internal reflection in the optical range.

The wave functions of the incident waves can be represented on the surface of the medium as

$$\exp\,(\mathrm{i}k_x x) \quad \text{and} \quad \exp\,[\mathrm{i}(k_x + \Delta k_x)x]\,.$$

Because the wavenumbers of these two waves are not the same, the phases of the reflected waves corresponding to them are also different. Therefore, the wave functions of the reflected waves are

$$\exp\,(\mathrm{i}k_x x + \mathrm{i}\varphi) \quad \text{and} \quad \exp\,[\mathrm{i}(k_x + \Delta k_x)x + \mathrm{i}(\varphi + \Delta\varphi)]\,.$$

The phases φ and $\varphi + \Delta\varphi$ can be determined in a standard way, by requiring the continuity of the wave functions and their derivatives along the direction normal to the interface of the two media. The waves interfere with each other, yielding a combined reflected wave

$$\Psi(x) = \exp\,(\mathrm{i}k_x x + \mathrm{i}\varphi)\Big\{1 + \exp\,\big[\mathrm{i}(\Delta k_x x + \Delta\varphi)\big]\Big\}\,. \tag{3}$$

The condition for the maximum reflected intensity, i.e., the constructive interference requirement, is

$$\Delta k_x x + \Delta\varphi = 2\pi\nu\,, \tag{4}$$

where ν is an integer.

If there is no TER, as is the case with neutrons with an energy $E_\mathrm{n} > U$ above the TER threshold, and absorption is disregarded, the phase shift does not appear, i.e., $\Delta\varphi = 0$. The maximum-intensity condition is represented in this case as $\Delta k_x x_0 = 2\pi\nu$. By comparing the maximum interference conditions in both cases, we can conclude that the phase shift accompanying TER results in shifting the beam along the x axis by $\xi = x - x_0 = -\Delta\varphi/\Delta k_x$. Taking the derivative, we obtain the well-known formula derived by Artmann [3] for the longitudinal GH shift:

$$\xi = -\frac{\mathrm{d}\varphi}{\mathrm{d}k_x}\,. \tag{5}$$

We have assumed that the wavenumber k_x only changes as a result of variation of the angle of incidence. Because $k^2 = k_x^2 + k_z^2$ is invariable, we express the shift ξ in (5) in terms of the derivative by the 'normal energy' E_n in (2):

$$\xi = \frac{\hbar^2 k_x}{m}\,\frac{\mathrm{d}\varphi}{\mathrm{d}E_\mathrm{n}}\,. \tag{6}$$

The phase φ of the wave reflected from the potential U can be derived in a standard way from the expression for the reflected wave amplitude:

$$r(k_z) = \frac{k_z - q_z}{k_z + q_z}\,, \tag{7}$$

where $q_z = \sqrt{k_z^2 - k_\mathrm{b}^2}$ is the z-component of the neutron wave vector in the medium and $k_\mathrm{b} = \sqrt{2mU}/\hbar$ is the boundary (critical) value of the wavenumber. Equation (7) and the TER

condition $|r(k_z)| = 1$ yield

$$\varphi = -\arcsin\left(\frac{2\sqrt{E_{\rm n}(U-E_{\rm n})}}{U}\right), \quad U > E_{\rm n}\,. \tag{8}$$

Finally, from (6) and (8), we obtain

$$\xi = \frac{2k_x}{k_z\sqrt{k_{\rm b}^2 - k_z^2}}\,, \quad k_z < k_{\rm b}\,, \tag{9}$$

in complete agreement with the results in [49].[1]

We note a distinguishing feature of Eqn (6). The factor

$$\tau = \hbar\frac{{\rm d}\varphi}{{\rm d}E_{\rm n}} \tag{10}$$

that it contains is the well-known group delay time (GDT) introduced by Eisenbud, Bohm, and Wigner [58–60] as a measure of the interaction time in quantum mechanics.[2] Therefore, Eqn (6) for the longitudinal GH shift can be represented as

$$\xi = \tau V_x\,, \tag{11}$$

where $V_x = \hbar k_x/m$ is the longitudinal (directed along the surface) component of neutron velocity.

The GDT in (10) can be identified, with some stipulations, with the neutron reflection time. Agudin [50] was the first to indicate a relation between the reflection time and the GH longitudinal shift.

Equation (11) can be interpreted in simple physical terms. The incident neutron beam enters the medium and reappears on the surface (is reflected). For this, it needs some time τ that depends on the medium structure, the neutron energy, the angle of incidence, etc. But because the wavenumber component k_x and the classical velocity V_x associated with it do not change on the interface between the media, the shift of the reflected beam is determined by the time the neutron stays in the medium. Equations (9) and (11) show that the time of reflection from a potential barrier U is

$$\tau = \frac{2m}{\hbar k_z\sqrt{k_{\rm b}^2 - k_z^2}} = \frac{\hbar}{\sqrt{E_{\rm n}(U-E_{\rm n})}}\,. \tag{12}$$

A different approach to the GH effect, which is based on the balance of fluxes for total internal reflection, was used by Renard [6]. We consider the basic concepts of that theory as applied to the reflection of a massive particle from a region where the potential is nonzero.

When there is TER, the wave penetrates into the region where the potential is nonzero and exponentially decreases there. This means that the density of particles in the classically forbidden region is finite and there is a corresponding flux of particles directed parallel to the interface (Fig. 1). This additional flux $J_x^{\rm t}$, which is a consequence of the partial penetration of the wave through the interface, must be compensated with a decrease in the flux in the region that corresponds to geometric reflection of the initial beam. Having calculated this excess flux, we can determine the transverse shift d (see Fig. 1) and the corresponding shift ξ along the interface.

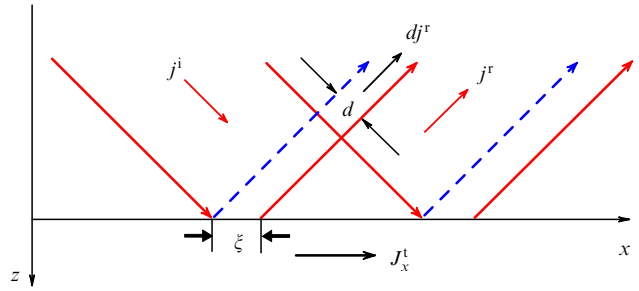

Figure 1. (Color online.) Illustration for the derivation of Eqn (18) for the longitudinal shift using the flux balance method [6].

In the region where the potential is nonzero, $z \geqslant 0$, the wave function is given by

$$\Psi_t(x,z) = t\exp\left({\rm i}k_x x - \chi z\right), \tag{13}$$

where t is the amplitude and χ is the absolute value of the imaginary-valued wave vector of the decreasing (evanescent) wave,

$$t = \frac{2k_z\left(k_z - {\rm i}\sqrt{k_{\rm b}^2 - k_z^2}\right)}{k_{\rm b}^2}\,, \quad \chi = \sqrt{k_{\rm b}^2 - k_z^2}\,. \tag{14}$$

The flux along the interface inside the medium is[3]

$$J_x^{\rm t} = V_x\int_0^\infty \left|\Psi_t(x,z)\right|^2 {\rm d}z\,. \tag{15}$$

Substituting Eqns (13) and (14) in (15), we obtain

$$J_x^{\rm t} = \frac{2\hbar}{m}\frac{k_x}{\sqrt{k_{\rm b}^2 - k_z^2}}\frac{k_z^2}{k_{\rm b}^2}\,. \tag{16}$$

The flux densities of the incident and reflected waves outside the overlap region can be presented as $j^{\rm i} = j^{\rm r} = \hbar k_0/m = V_0$, where $k_0 = \sqrt{k_x^2 + k_z^2}$. Equating the reflected wave flux $J^{\rm r} = dj^{\rm r}$ in a strip with a width d to the flux inside matter $J_x^{\rm t}$ in (16), we find the beam shift d in the direction perpendicular to the direction of the reflected wave propagation (see Fig. 1):

$$d = \frac{k_x}{k_0 k_{\rm b}^2}\frac{2k_z^2}{\sqrt{k_{\rm b}^2 - k_z^2}}\,. \tag{17}$$

Because the shift along the surface is $\xi = (k_0/k_z)d$, we obtain the Renard formula [6] for the GH shift:

$$\xi = \frac{2k_x k_z}{k_{\rm b}^2\sqrt{k_{\rm b}^2 - k_z^2}}\,. \tag{18}$$

Equation (18) differs from Artmann–Carter–Hora formula (9) and is not in line with the understanding of the relation between the GH shift ξ in (11) and the GDT τ; this circumstance, however, did not prevent this result from becoming widely acknowledged. Shortly afterwards, this result was confirmed by Lotsch [7]. The authors of [52] used

[1] Equation (9) coincides with Eqn (27) in [49] if the wavelength and angle of incidence are replaced in the latter formula with wave vector components; however, it differs from Eqn (1) in [49], which contains a typo.

[2] For a long time, it was referred to as the phase-delay time.

[3] Given the 2D nature of the problem, here and below the term 'flux' means a flux in a unit-width strip along the y axis.

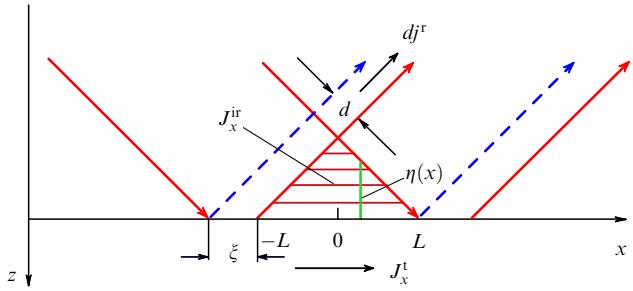

Figure 2. (Color online.) Illustration for the derivation of Eqn (9) for a longitudinal shift using the flux balance method with the flux in the wave overlap region taken into account [15].

Eqn (18) to estimate the GH effect in the neutron experiments they had proposed, while the authors of [54] compared their experimental results to that formula.

The reason why the two physical approaches yielded incompatible results remained unclear for a long time. It was no less than 20 years after Renard's study [6] that Yasumoto and Oishi [15] and Fedoseyev [17] published papers where the paradox was resolved. The point is that Renard's approach [6] assumes that the total reflection only differs from the ideal geometric reflection by the presence of a flux of evanescent waves in the medium. The author overlooked the fact that due to a nonzero phase difference between the incident and reflected waves, the flux is also distorted in regions where those waves overlap (Fig. 2), while in Artmann's approach [3], as was shown above, the GH effect is caused by the phase shift that occurs for total reflection.

We show, following [15], how taking this circumstance into account affects the result. In the region where the incident and reflected waves overlap, the wave function is

$$\Psi^{\mathrm{ir}}(x,z) = \exp\left[\mathrm{i}(k_x x + k_z z)\right] + r\exp\left[\mathrm{i}(k_x x - k_z z)\right]. \quad (19)$$

In the case of TER from a potential barrier and the absence of absorption, the reflected-wave amplitude is $r = \exp(\mathrm{i}\varphi)$, where the phase φ follows from Eqn (8).

Calculation of the flux density $j_x^{\mathrm{ir}}(z) = V_x\left|\Psi^{\mathrm{ir}}(x,z)\right|^2$ along the x axis in the wave overlap region under consideration yields

$$j_x^{\mathrm{ir}}(z) = 2V_x\left[1 + \cos(2k_z z - \varphi)\right]. \quad (20)$$

To calculate the flux J_x^{ir}, this density must be integrated over the entire region where the beams overlap (see Fig. 2). Following the approach of Yasumoto and Oishi [15], we assume that the base of the triangular region where the beams overlap is limited by the points $x = -L$ and $x = L$, while the profile height $\eta(x) = (|x| - L)k_z/k_x$ of this region depends on the current coordinate x $(-L < x < L)$:

$$J_x^{\mathrm{ir}} = \lim_{L\to\infty}\left[\frac{1}{2L}\int_{-L}^{L}\left(\int_{\eta(x)}^{0} j_x^{\mathrm{ir}}(z)\,\mathrm{d}z\right)\mathrm{d}x\right]. \quad (21)$$

The first integration over the coordinate z in (21) yields

$$\int_{\eta(x)}^{0} j_x^{\mathrm{ir}}(z)\,\mathrm{d}z = -2V_x\left\{\eta(x) + \frac{1}{2k_z}\left[\sin\left(2k_z\eta(x) - \varphi\right) + \sin\varphi\right]\right\}. \quad (22)$$

Subsequent integration over x of the first integrand in (22) yields the flux $I_0 = V_x H$, where $H = (k_z/k_x)L$ is the maximum height of the triangular region where the waves overlap. This would be the value of the flux if the reflected wave had no phase shift that emerges due to TER. The integral of the second oscillating integrand in (22) vanishes if the interval $(-L, L)$ is extended to a size larger than the wavelength. The remaining integral

$$J_x^{\mathrm{int}} = -\frac{V_x}{k_z}\sin\varphi, \quad (23)$$

which is added to the flux $I_0 = V_x H$, is the measure of the flux distortion in the interference region of the overlapping beams due to TER and the phase shift φ related to it.

Thus, the excess flux ΔJ due to the TER is a sum of the flux J_x^{t} in (16) of the wave evanescing in the potential region and the flux J_x^{int} in (23) related to the interference of the incident and reflected waves. Given formula (8) for the phase shift φ, we obtain

$$\Delta J = J_x^{\mathrm{t}} + J_x^{\mathrm{int}} = \frac{2\hbar k_x}{m\sqrt{k_{\mathrm{b}}^2 - k_z^2}}. \quad (24)$$

Using the condition $\Delta J = dj^{\mathrm{r}}$ for the transverse beam shift $d = \Delta J/V_0$, we find

$$d = \frac{2k_x}{k_0\sqrt{k_{\mathrm{b}}^2 - k_z^2}}. \quad (25)$$

Using this formula, we obtain the result (9) for the GH shift $\xi = (k_0/k_z)d$.

Thus, the approach based on the balance of fluxes yields a result that is exactly the same as in Artmann's method [3]. Moreover, it enables the reflection time to be determined in a somewhat different way [15]. Indeed, being finite, the reflection time τ results in an excess of neutrons $N = \Delta J/V_x$, where the flux ΔJ is determined by Eqn (24). Having divided N by the normal component of the incident flux density V_z, we obtain the reflection time in exactly the same form as follows from (12).

Because the typical value of the effective potential U in Eqn (1) is of the order of 100–250 neV and the total external reflection is only possible if $E_{\mathrm{n}} < U$, Eqn (12) shows that except for two narrow regions close to zero energy and the threshold, the group delay time for reflected neutrons is $\tau \approx 5-30$ ns. For example, if the neutron velocity is $V_x \approx 10$ m s^{-1} and the GDT is $\tau \approx 10$ ns, the longitudinal GH shift is $\xi \approx 100$ nm.

3. Giant positive and negative longitudinal shifts of the reflected beam in the plane-wave approximation

Direct observation of the neutron beam shift under TER is a rather difficult task. The difficulty is due not only to the tiny size of the effect but also to the absence of a point from which that shift might be measured. In their pioneering experiments [1, 2], Goos and Hänchen compared the position of a wave beam that exhibited internal reflection with the position of a beam reflected from a metal film. It was assumed that if the beam is reflected from metal, no wave shift occurs; however, this assumption is not quite true [25]. It is difficult to design such a 'zero experiment' for neutron beams. It was proposed

in [51, 52] to compare the actual position of the beam with the calculated one, and in [52], to measure the phase of the reflected wave using a neutron interferometer. However, the phase shift of the reflected wave and the effect of the longitudinal shift are physically different, even if closely related phenomena. Therefore, it is not quite correct to interpret the visual manifestation of the phase effects for bounced neutrons found in [54] as an observation of the GH shift (see the discussion in [55, 56]).

To resolve the problem, it was proposed in [57] to implement the idea of resonant enhancement of the shift for waves reflected from multilayer structures; Tamir and Bertoni [61] were the first to propose it for light beams. The problem was studied later theoretically in [62–64], and a large shift for the waves reflected from a multilayer waveguide structure was observed in [65, 66]. A similar proposal applied to neutrons was considered from a somewhat different standpoint in [53].

The conditions for the waveguide-type propagation of a neutron flux along the medium boundary seem to hold for a vast variety of planar structures. The simplest structure of this type consists of a homogeneous film with an effective potential U_1 overlaying a substrate with a potential $U_2 > U_1$. The general expression for the amplitude of the reflected wave $r(E_n)$ is given, for example, in [57]. It is obvious that neutrons with the energy $E_n < U_2$ exhibit total reflection from that structure, and $r = \exp(i\varphi)$. Having calculated the reflected wave phase $\varphi = \arctan(\mathrm{Im}\, r/\mathrm{Re}\, r)$, we can easily calculate the derivative $d\varphi/dE_n$ and GDT (10), which is directly related to longitudinal shift (11). Figure 3 shows the results of that calculation for a 90 nm thick silver film with the effective potential $U_1 = 91$ neV on a nickel substrate with $U_2 = 245$ neV.

As follows from Fig. 3a, the GDT (curve *1*) in resonance attains the maximum value $\tau_m = 260$ ns for the neutron energy $E_n = 109$ neV. We note, however, that GDT (12) for the reflection from the potential U_2 in the absence of a film is 5.4 ns. The reflection phase (Fig. 3b) increases monotonically as the energy increases, and hence its derivative is always positive and $\tau > 0$. It follows from (11) that the longitudinal shift of the reflected beam exhibits the same resonant growth as the GDT.

There is another noticeable phenomenon that can be observed in the reflection of neutrons from multilayer structures. Under some conditions, the GDT and the longitudinal shift of the reflected beam can be negative. The possibility that the GH shift for an optical beam might be negative was indicated for the first time in study [61] cited above. The negative shift of the optical beam and a negative GDT have been explored in numerous theoretical [61–67] and experimental [72–75] studies. There are sufficiently many objects and media for which the reflected beam has a negative shift; in some cases, it is indeed generated by a flux propagating in the negative direction (see, e.g., [72]). A detailed review of corresponding publications is beyond the scope of this paper, and we only consider the reflection of neutrons from the multilayer planar structure that was mentioned above.

We study the simplest structure of that kind: a uniform film covering a substrate. We consider the case where the hierarchy of the potentials is reversed, i.e., the potential U_1 of the film is larger than the potential U_2 of the substrate. The effective potential representing this structure has the shape of an asymmetric barrier. The coefficient of reflection from that

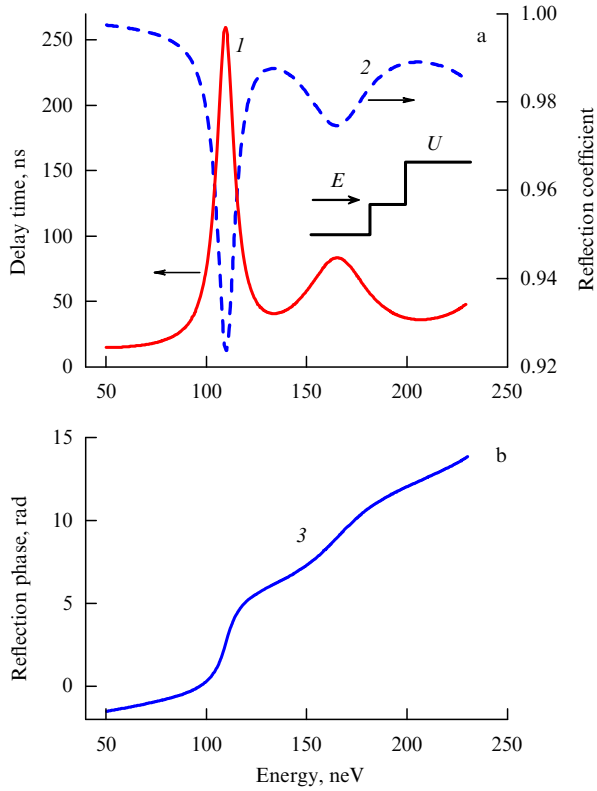

Figure 3. Group delay time (curve *1*), reflection coefficient (curve *2*), and phase (curve *3*) for neutrons reflected from a silver film with thickness $l = 90$ nm on a nickel substrate. The inset shows the potential $U(z)$ of that sample. The GDT attains the maximum $\tau_m = 260$ ns for the neutron energy $E_n = 109$ neV.

barrier $R(E_n) = |r(E_n)|^2$ can easily be calculated. Above the barrier, i.e., for the energy $E_n > U_1$, it is oscillating and rapidly decreasing. The group time for the wave reflection from an asymmetric potential barrier was found in [76]. The study showed that at transmission resonances, i.e., at the reflection curve minima, the group reflection time is negative. According to (11), the reflected beam must exhibit a negative spatial shift under those conditions.

Figure 4a shows the calculated GDT (curve *1*) and the neutron reflection coefficient (curve *2*) for a 100 nm thick nickel film overlaying a silver substrate. It can be seen that the group time attains large negative values at the minima of reflection curve *2* ($\tau_m = -541$ ns for the energy $E_n = 265$ neV). The reflection phase (Fig. 4b) is oscillating and contains segments where its derivative and hence the GDT are negative. Although the reflection coefficient is not large, we can expect that the manifestations of that negative time and negative longitudinal shift of the beam can be measurable.

The variety of possible multilayer structures that have a negative GDT is rather broad. Owing to this, one can choose the optimal relation between the absolute value of the delay time and the intensity of the reflected beam.

As an example, calculations for a three-layer structure whose effective potential is given by two barriers of unequal width and a well separating them were reported in [57]. An analytic solution for the reflection and transmission amplitudes for that structure was found in [77], and the tunneling of particles through a double-peaked barrier was studied in [78].

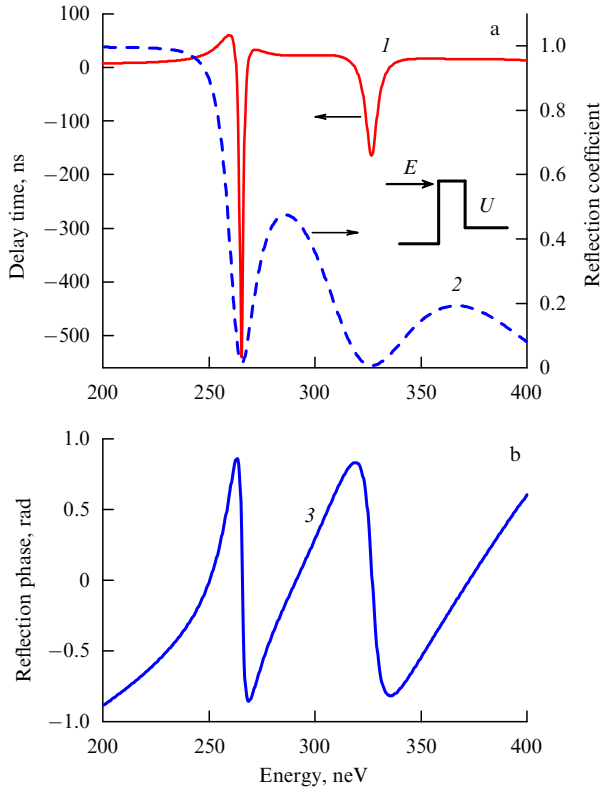

Figure 4. Group delay time (curve *1*), reflection coefficient (curve *2*), and phase (curve *3*) for neutrons reflected from an asymmetric barrier created by a thin nickel film with thickness $l = 100$ nm on a silver substrate. The inset shows the potential $U(z)$ of that sample. The GDT attains the negative value $\tau_m = -541$ ns for the neutron energy $E_n = 265$ neV.

The structure considered in [57] consisted of Ni–Ti–Ni films with the respective thicknesses 23, 13, and 33 nm. The calculated phase of the reflected wave and the neutron delay time are shown in Fig. 5. It is noteworthy that the results strongly depend on the direction in which the wave is incident on that structure. If the wave propagates from the side of the thinner barrier, the reflection phase monotonically increases (Fig. 5c), and therefore the GDT is positive, attaining the value $\tau_m = 377$ ns (Fig. 5a, curve *1*). If the wave propagates from the opposite direction, the GDT is negative ($\tau_m = -80$ ns; Fig. 5b, curve *1*). The reflection phase has in this case an S-like shape (Fig. 5d) with a negative derivative close to the energy $E_n \approx 144$ neV. At the same time, the absolute values of the reflection and transmission coefficients (with absorption ignored) are independent of the direction of propagation. The reflection coefficient at the resonance is about 40%, and the absolute value of the negative GDT is in this case about five times smaller than in the preceding case.

Thus, a simple calculation for a number of planar resonance structures shows that the group delay time can be negative. We recall that in the case of TER, the reflected wave shift and the GDT proportional to it are related to the neutron flux along the interface of the media. However, the flux propagating in the negative direction is not traceable in the examples discussed above. Therefore, the phenomenon or paradox of a negative GDT for neutrons and the negative GH effect requires an explanation.

We emphasize that the results discussed above have been obtained in the approximation of plane waves, which are infinite by definition. This problem therefore requires a more accurate study, which is presented in Section 4.

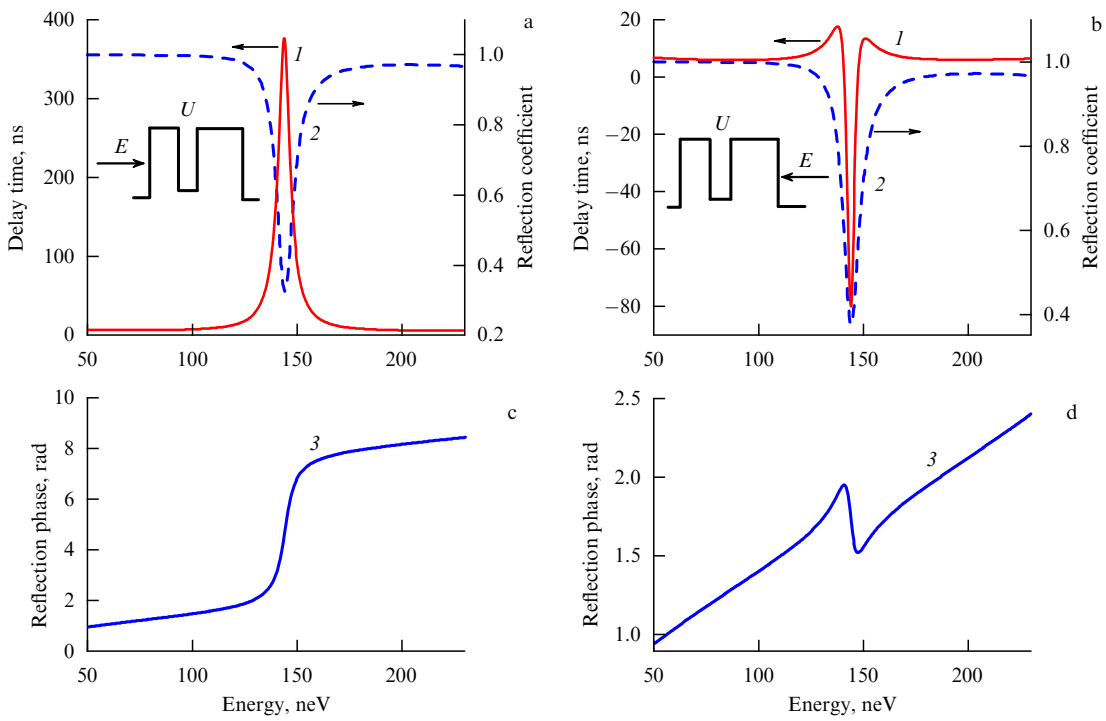

Figure 5. (a, b) Group delay time (curves *1*), reflection coefficient (curves *2*) and (c, d) reflection phase (curves *3*) for an asymmetric structure consisting of two barriers and a well between them. The shape of the potential and wave propagation direction are shown in the inset; the resonance corresponds to the neutron energy $E_n \approx 144$ neV; the GDT is $\tau_m \approx 377$ ns in (a) and $\tau_m \approx -80$ ns in (b).

4. Goos–Hänchen shift and the time of reflection of a bounded neutron beam from matter

4.1 General relations

In this section, we study the reflection of a monochromatic spatially bounded and stationary neutron beam from the interface between a vacuum and an arbitrary structure.

We consider the neutrons incident on a medium at a glancing angle θ. The projections of the wave vector $\mathbf{k}_0$ are $k_{0x} = k_0 \cos\theta$ and $k_{0z} = k_0 \sin\theta$, where the x axis is directed, as before, along the interface and the z axis is perpendicular to the interface and directed into the medium.

We assume that the beam is formed using a set of slits, whose boundaries are not necessarily sharp. The wave function of the neutron beam incident on the medium can be represented as

$$\Psi_{\text{in}}(\mathbf{r}) = A_{\text{in}}(\mathbf{r}) \exp(\mathrm{i}\mathbf{k}_0\mathbf{r}), \tag{26}$$

where $A_{\text{in}}(\mathbf{r})$ is generically a slowly varying complex-valued amplitude of the beam with a characteristic transverse size $r_0 \gg \lambda_0$. At the interface $z = 0$, we have

$$\Psi_{\text{in}}(x) = A_{\text{in}}(x) \exp(\mathrm{i}k_{0x}x). \tag{27}$$

To solve the problem of beam reflection, we use the plane-wave expansion method, well known in wave optics (see, e.g., [79]). We represent the wave function amplitude $A_{\text{in}}(x)$ in (27) on the surface as a Fourier integral

$$A_{\text{in}}(x) = \int_{-\infty}^{\infty} A_{\text{in}}(q) \exp(\mathrm{i}qx)\, \mathrm{d}q, \tag{28}$$

where spectral–angular components (amplitudes) are given by the inverse Fourier transformation:

$$A_{\text{in}}(q) = \frac{1}{2\pi}\int_{-\infty}^{\infty} A_{\text{in}}(x) \exp(-\mathrm{i}qx)\, \mathrm{d}x. \tag{29}$$

Substituting (28) in (27), we obtain an expression for the wave function $\Psi_{\text{in}}(x)$ on the surface:

$$\Psi_{\text{in}}(x) = \int_{-\infty}^{\infty} A_{\text{in}}(q) \exp\left[\mathrm{i}(k_{0x} + q)x\right] \mathrm{d}q. \tag{30}$$

The last equation can be interpreted as an infinite set of plane waves with amplitudes $A_{\text{in}}(q)$ and projections of wave vectors

$$k_x = k_{0x} + q, \quad k_z = \sqrt{k_0^2 - (k_{0x} + q)^2}. \tag{31}$$

Equation (31) shows that the boundedness of the beam results in distributions of wave vector projections in both longitudinal and transverse directions. The function $A_{\text{in}}(q)$ attains a maximum at $q = 0$ and decreases as q increases. The width of this function is $\Delta q \approx 1/r_0$, and hence the angular spectrum width diminishes if the cross section of the beam increases.

To find the amplitude of the reflected beam $A_{\text{R}}(x)$ on the surface $z = 0$, we multiply the amplitude of each plane wave that forms the incident beam by the corresponding amplitude reflection coefficient $r(k_x)$. As a result, we obtain

$$A_{\text{R}}(x) = \int_{-\infty}^{\infty} A_{\text{in}}(q) r(k_{0x} + q) \exp(\mathrm{i}qx)\, \mathrm{d}q. \tag{32}$$

Equation (32) shows that the reflected beam shifts along the x axis with respect to the incident beam, and its shape differs from the original profile $A_{\text{in}}(x)$.

The validity of the first conclusion can be easily illustrated in the following way. We represent the amplitude reflection coefficient $r(k_x)$ in the form

$$r(k_{0x} + q) = \left|r(k_{0x} + q)\right| \exp\left[\mathrm{i}\varphi(k_{0x} + q)\right], \tag{33}$$

where $\varphi(k_{0x} + q)$ is the phase of the amplitude reflection coefficient of the plane wave with the wave vector projection $k_x = k_{0x} + q$. We also assume that within the angular spectrum width Δq, the variation in the absolute value of the reflection coefficient is negligible, i.e., $\left|r(k_{0x} + q)\right| \approx \left|r(k_{0x})\right|$. We expand the reflection coefficient phase in a Taylor series and keep the first two terms:

$$\varphi(k_{0x} + q) \approx \varphi(k_{0x}) + \frac{\mathrm{d}\varphi}{\mathrm{d}k_x}\, q. \tag{34}$$

Substituting (34) in (32) with the conclusion regarding the absolute value of the reflection coefficient taken into account yields the result

$$A_{\text{R}}(x) = \left|r(k_{0x})\right| \exp\left[\mathrm{i}\varphi(k_{0x})\right] \times \int_{-\infty}^{\infty} A_{\text{in}}(q) \exp\left[\mathrm{i}q\left(x + \frac{\mathrm{d}\varphi}{\mathrm{d}k_x}\right)\right] \mathrm{d}q. \tag{35}$$

Using Eqn (28) for $A_{\text{in}}(x)$, we obtain the absolute value of the plane wave amplitude

$$\left|A_{\text{R}}(x)\right| = \left|r(k_{0x})\right| \left|A_{\text{in}}(x - \xi)\right|, \tag{36}$$

where

$$\xi = -\frac{\mathrm{d}\varphi}{\mathrm{d}k_x}. \tag{37}$$

Thus, Eqn (36) shows that within the adopted approximations and according to the conclusions drawn above, the beam shifts as a whole along the interface by the quantity ξ in Eqn (37); its shape (profile) remains the same as that of the incident beam, and its amplitude is multiplied by a constant factor, the absolute value of the amplitude reflection coefficient $\left|r(k_{0x})\right|$.

Two important comments are relevant here. First, the value of the longitudinal shift is determined by the derivative of the reflection coefficient phase $r(k_x)$ rather than the derivative of the reflected beam phase, which can in general depend on the phase distribution in the incident beam. This circumstance is ignored in the plane-wave approximation. Second, the conclusion that the beam profile does not change originates from approximation (34) made above. If the next terms in expansion (34) are taken into account and, moreover, integral (32) is calculated more accurately, this conclusion is longer valid [11, 36, 46, 47, 79].

4.2 Reflection of a Gauss beam with a quadratic phase dependence

In studying the reflection of a beam from an interface, it is not infrequent that the amplitude $A_{\text{in}}(x)$ is assumed to be real-valued and to have the form of a rectangular step ($A_{\text{in}}(x) = 1$ for $|x| \leqslant r_0$ and $A_{\text{in}}(x) = 0$ for $|x| > r_0$) or a Gaussian beam with the profile $A_{\text{in}}(x) = \exp(-x^2/2r_0^2)$. It is easy to show

that the Fourier amplitudes $A_{\rm in}(q)$ in (29) are then symmetric real-valued functions.

However, in the case of both a slit and a Gaussian beam, the wave amplitude $A(x)$ at an arbitrary distance z from the source typically has complex values, and the phase of that amplitude has a quadratic dependence on the transverse coordinate x. This can be shown in the simplest way using the Green's function for free space $G(x,z) = (1/R)\exp(\mathrm{i}k_0R)$, where $R = \sqrt{x^2+z^2}$. At a sufficiently long distance $z \gg x$, the wave phase is $k_0R \approx k_0z + k_0x^2/(2z)$, where the first term is the plane-wave phase and the second term, which is quadratic in the transverse coordinate x, describes the parabolic wave-front curving, i.e., the well-known phenomenon of the angular divergence of radiation.

We support these qualitative conclusions with an accurate calculation for the Gaussian beam, for which simple analytic expressions can be derived.

We assume that in the plane $z = 0$ we have a wave function with a real-valued amplitude $A(x,0) = \exp[-x^2/(2r_0^2)]$. The solution of the wave equation $\Delta\Psi + k_0^2\Psi = 0$ in a vacuum in an arbitrary plane z has the general form

$$\Psi(x,z) = \int_{-\infty}^{\infty} A(q)\exp\left(\mathrm{i}qx + \mathrm{i}\sqrt{k_0^2-q^2}\,z\right)\mathrm{d}q\,, \qquad (38)$$

where, according to (29),

$$A(q) = \frac{r_0}{\sqrt{2\pi}}\exp\left(-\frac{q^2r_0^2}{2}\right). \qquad (39)$$

In the paraxial approximation $q \ll k_0$, the expansion $(k_0^2-q^2)^{1/2} \approx k_0 - q^2/(2k_0)$ holds. From (38) and (39), we then obtain the wave function at the observation point $\Psi(x,z) = A(x,z)\exp(\mathrm{i}k_0z)$, where the amplitude varies slowly and is given by

$$A(x,z) = \frac{1}{\sqrt{1+\mathrm{i}D}}\exp\left(-\frac{x^2}{2r_1^2} + \mathrm{i}\varphi(x,z)\right). \qquad (40)$$

Here, $D = \lambda_0 z/(\pi r_0^2)$ is the so-called wave parameter [79], while the characteristic beam size $r_1(z)$, which exhibits diffraction broadening as the distance z increases, and the phase $\varphi(x,z)$ are defined as

$$r_1(z) = r_0\sqrt{1+D^2}\,, \quad \varphi(x,z) = \frac{D}{1+D^2}\,\frac{x^2}{2r_0^2}\,. \qquad (41)$$

Finally, we obtain a generalized form of the complex-valued amplitude of the Gaussian beam:

$$A(x) = \exp\left[-\frac{x^2}{2r_0^2}(1-\mathrm{i}\alpha_0)\right], \qquad (42)$$

where α_0 is a dimensionless parameter of the quadratic phase on a plane that can be considered the radiation source plane. From Eqns (29) and (42), we obtain that the Fourier amplitude of such a beam is independent of the distance z from the source, is a complex-valued function (for $\alpha_0 \neq 0$), and is given by [cf. Eqn (39)]

$$A(q) = \frac{r_0}{\sqrt{2\pi(1-\mathrm{i}\alpha_0)}}\exp\left[-\frac{q^2r_0^2}{2(1+\alpha_0^2)}(1+\mathrm{i}\alpha_0)\right]. \qquad (43)$$

The spectrum $S(q)$ of that beam in the conjugate space, i.e., the space of wave vectors, is $S(q) = \left|A(q)\right|^2$. It is proportional to $\exp(-q^2/\Delta q^2)$, where $\Delta q = (1/r_0)\times(1+\alpha_0^2)^{1/2}$ is the spectrum half-width at the e^{-1} level. The angular spectrum width $\Delta\theta = \Delta q/k_0$ can be presented as

$$\Delta\theta = \frac{\lambda_0}{2\pi r_0}\sqrt{1+\alpha_0^2}\,. \qquad (44)$$

It is determined by both the diffraction width $\lambda_0/(2\pi r_0)$, which depends on the relation between the wavelength and the beam size on the initial plane $z = 0$, and the quadratic phase parameter α_0, which is determined by the prehistory of beam formation in the region $z < 0$.

In this section, we considered a plane that is perpendicular to the beam propagation along the z axis. If the beam is incident on the interface at a glancing angle, this can be taken into account by replacing the characteristic size of the beam r_0 in the equations above with $r_{0x} = r_0/\sin\theta$.

4.3 Reflection of neutron pulses of finite duration

We consider the important problem of the time delay of reflected neutron pulses in more detail. The most straightforward approach is to analyze time relations for a finite-duration neutron pulse reflected from a medium. Temporarily ignoring the longitudinal shift of the beam, we consider the simplest case of an incident neutron pulse that is not bounded in the transverse direction (a wave packet) and has a wave function $A_{\rm in}(z,t)$, where z is the axis directed into the medium and t is the time. The problem is to find the wave function $A_{\rm R}(z,t)$ of the reflected pulse.

We represent the wave function of the incident pulse in the $z = 0$ plane as

$$A_{\rm in}(t) = A_0(t)\exp(-\mathrm{i}\omega_0 t)\,, \qquad (45)$$

where $A_0(t)$ is the pulse envelope and ω_0 is the so-called central frequency, which is standardly related to the central energy $E_0 = \hbar\omega_0$, the velocity $V_0 = (2\hbar\omega_0/m)^{1/2}$, and the wave number $k_0 = (2m\omega_0/\hbar)^{1/2}$. The intensity of the incident pulse is $I_{\rm in}(t) = \left|A_0(t)\right|^2$. It is obvious that in forming a pulse of finite duration, we automatically assume that the incident state is characterized by an energy spectrum. Representation (45) for the pulse is valid if $\tau_0\omega_0 \gg 1$, where τ_0 is the characteristic duration of the pulse with a slowly varying amplitude $A_0(t)$.

We decompose wave function (45) in a Fourier integral,

$$A_{\rm in}(t) = \int_{-\infty}^{\infty} A_{\rm in}(\omega)\exp(-\mathrm{i}\omega t)\,\mathrm{d}\omega\,, \qquad (46)$$

where the so-called spectral amplitudes (and, below, the spectrum) are determined by the inverse Fourier transformation:

$$A_{\rm in}(\omega) \equiv A_0(\Omega) = \frac{1}{2\pi}\int_{-\infty}^{\infty} A_0(t)\exp(\mathrm{i}\Omega t)\,\mathrm{d}t\,, \qquad (47)$$

where $\Omega = \omega - \omega_0$.

Let $r(\omega)$ be the amplitude reflection coefficient of a plane monochromatic wave with a frequency ω, which is complex in general. The amplitude (envelope) of the wave function of the pulse reflected in the plane $z = 0$ is described by the simple equation

$$A_{\rm R}(t) = \int_{-\infty}^{\infty} A_0(\Omega)r(\omega_0+\Omega)\exp(-\mathrm{i}\Omega t)\,\mathrm{d}\Omega\,. \qquad (48)$$

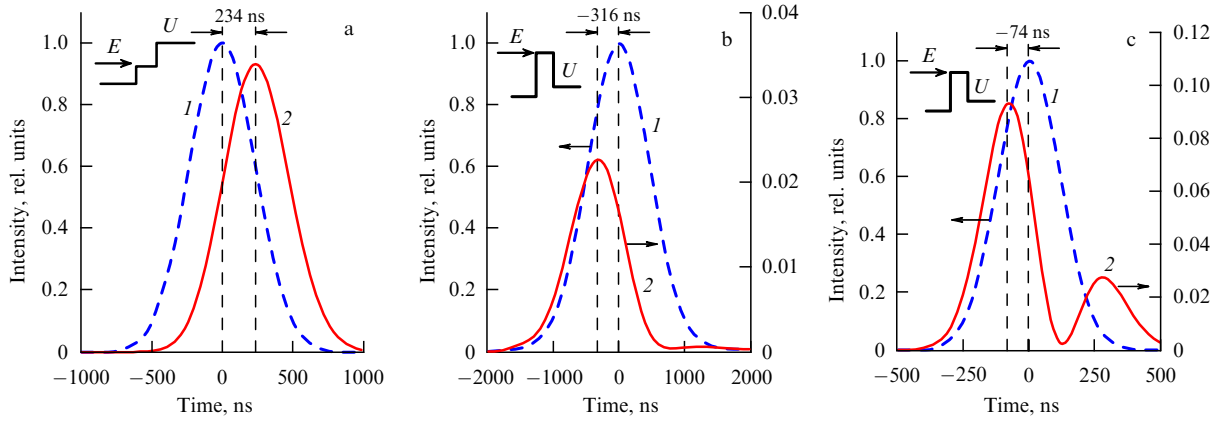

Figure 6. Amplitude and time relations between the intensities of incident (curves *1*) and reflected (curves *2*) neutron pulses. (a) Total reflection, incident pulse duration $\tau_0 = 330$ ns ($\Delta E = 2$ neV), reflected pulse shift $\Delta t = 234$ ns, GDT $\tau_m = 260$ ns. Over-barrier resonant reflection for (b) the incident pulse durations $\tau_0 = 660$ ns ($\Delta E = 1$ neV), $\Delta t = -316$ ns, $\tau_m = -541$ ns and (c) $\tau_0 = 165$ ns ($\Delta E = 4$ neV), $\Delta t = -74$ ns, $\tau_m = -541$ ns.

Equation (48) is a solution of the problem of pulse reflection from any structure that is characterized by the spectral reflection coefficient $r(\omega)$. The intensity of the reflected pulse is $I_R(t) = |A_R(t)|^2$.

We note that the reflection coefficient r, which is determined from the requirement of the continuity of the wave function and its first derivative along the coordinate z at the interfaces, is frequently expressed in neutron optics as a function of the normal projection of the incident wave vector k_z.[4] However, we can easily replace k_z with the corresponding 'normal' frequencies ω_n using the relation $\omega_n = \hbar k_z^2/(2m)$.

We represent the amplitude reflection coefficient $r(\omega)$ in the form

$$r(\omega) = |r(\omega)| \exp\left(\mathrm{i}\varphi(\omega)\right) \tag{49}$$

and consider the case where the absolute value of the reflection coefficient varies weakly within the limits of the incident pulse energy spectrum. We can then set $|r(\omega)| \approx |r(\omega_0)|$ and take this factor outside the integral in (48). We expand the phase $\varphi(\omega_0 + \Omega)$ of the reflection coefficient in a series in the frequency Ω:

$$\varphi(\omega) = \varphi(\omega_0) + \varphi'(\omega_0)\Omega + \frac{1}{2}\varphi''(\omega_0)\Omega^2\,, \tag{50}$$

where $\varphi'(\omega_0) = (\mathrm{d}\varphi/\mathrm{d}\omega)|_{\omega_0}$ is the first derivative of the phase of the amplitude reflection coefficient and φ'' is its second derivative. For comparison with previous results for the longitudinal GH shift, we keep only the first-order term in Ω and insert (50) into (48). We then obtain

$$A_R(t) = |r(\omega_0)| \exp\left[\mathrm{i}\varphi(\omega_0)\right] \int_{-\infty}^{\infty} A_0(\Omega) \exp\left[-\mathrm{i}\Omega(t-\tau)\right] \mathrm{d}\Omega\,, \tag{51}$$

where the time shift

$$\tau = \left.\frac{\mathrm{d}\varphi}{\mathrm{d}\omega}\right|_{\omega_0} \tag{52}$$

coincides with the definition of the GDT in (10).

[4] It is only possible if Eqn (1) and the corresponding dispersion law $k^2 = k_0^2 - k_b^2$ are valid.

In comparing (51) and (46), we see that the envelope of the reflected pulse, up to an insignificant phase, is the incident pulse envelope, but is time shifted by a 'delay time' τ, Eqn (52), and multiplied by the absolute value of the reflection coefficient at the frequency ω_0:

$$|A_R(t)| = |r(\omega_0)|\,|A_0(t-\tau)|\,. \tag{53}$$

If the derivative with respect to the phase in (52) is positive, the pulse is reflected with some time delay. This phenomenon seems to be quite natural, because the pulse needs some time to propagate in direct and inverse directions in the medium.

If the derivative is negative, we obtain a physically impossible result: the pulse is reflected (or reflection begins) even before the incident pulse reaches the surface of the medium. We have shown above that the situation with a negative-valued derivative (10) is observed in many cases.

This paradox apparently occurs because general formula (48) is oversimplified as a result of expansion of the phase in series (50). We recall that the GDT concept was introduced in the classical work of Bohm and Wigner [59, 60], where they considered an example of single scattering of an incident quantum particle on another particle. If a wave is reflected from a macroscopic object, the effect of collective interaction of incident radiation with the medium has to be taken into account; this effect results, in particular, in a more complex energy dependence of the reflection phase. Therefore, the equation for GDT (10) is nothing more than a guiding estimate, and, to obtain the correct result, the spectral dependences of the functions $A_0(\Omega)$ and $r(\omega)$ in the integrand in (48) must be accurately taken into account.

Figures 6 and 7 show calculations of integral (48) for the reflection of neutrons from planar structures similar to those considered above. It was assumed in the calculations that incident pulse (45) has a Gaussian shape:

$$A_0(t) = \exp\left(-\frac{t^2}{2\tau_0^2}\right), \tag{54}$$

where τ_0 is the pulse duration. The zero-time reference was chosen in such a way that the pulse maximum at $t = 0$ corresponds to the maximum on the medium surface $z = 0$.

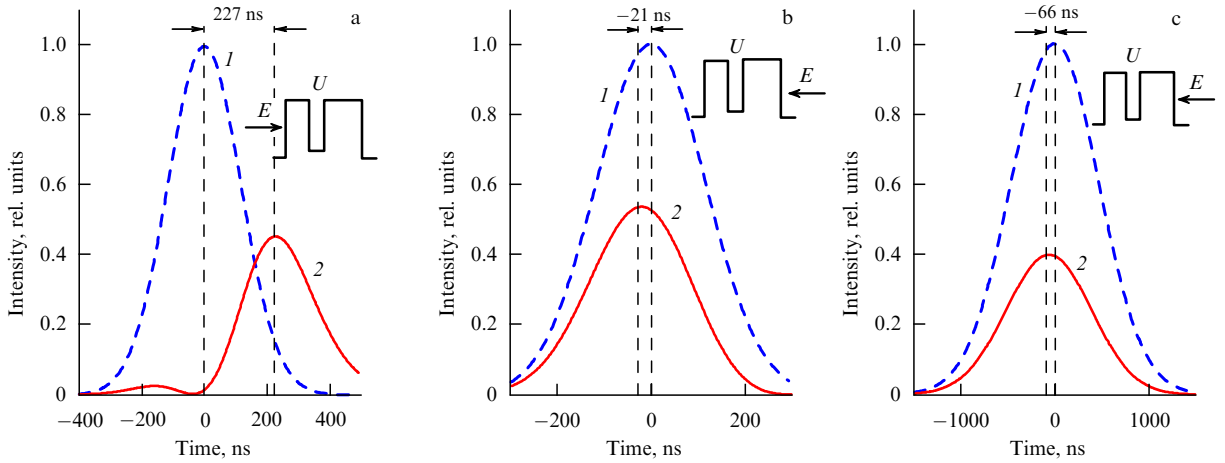

Figure 7. Amplitude and time relations between the intensities of incident (curves *1*) and reflected (curves *2*) neutron pulses for an asymmetric three-layer structure Ni(23 nm)/Ti(13 nm)/Ni(33 nm). The resonance energy of neutrons is $E_n = 144$ neV; (a) incident pulse duration $\tau_0 = 165$ ns ($\Delta E = 4$ neV), reflected pulse shift $\Delta t = 227$ ns, ideal GDT $\tau_m = 377$ ns; (b) $\tau_0 = 165$ ns, $\Delta t = -21$ ns, $\tau_m = -80$ ns; (c) $\tau_0 = 660$ ns ($\Delta E = 1$ neV), $\Delta t = -66$ ns, $\tau_m = -80$ ns.

The following formula is then valid for the frequency spectrum determined by integral (47):

$$A_0(\Omega) = \frac{1}{\Delta\Omega\sqrt{2\pi}} \exp\left(-\frac{\Omega^2}{2\Delta\Omega^2}\right), \tag{55}$$

where $\Delta\Omega = 1/\tau_0$ is the pulse spectrum width determined by its duration τ_0. This model apparently assumes that the pulse is fully coherent, i.e., is a statistically nonrandom regular wave packet. This model is well suited for explaining the physics of the phenomenon, but it can hardly be used to correctly describe results of a real experiment.

Figure 6a shows the shape and relative position of the incident (curve *1*) and reflected (curve *2*) pulses for a wave reflected from a planar structure consisting of a thin silver film on a nickel substrate. The parameters of the structure are the same as those in the caption to Fig. 3. The neutron energy $E_n = 109$ neV is smaller than the effective potential of the substrate $U_{Ni} = 245$ neV (the case of TER), and the pulse duration is $\tau_0 = 330$ ns, which corresponds to the energy spectrum width $\Delta E = 2$ neV. We can see that the maximum of the reflected wave packet (curve *2*) is shifted to the right by $\Delta t = 234$ ns, in correspondence to the real time delay. This value is close to the maximum GDT value $\tau_m = 260$ ns obtained in plane-wave approximation (10) (see Section 2).

Figures 6b and 6c show the time transformation of the pulse for resonant reflection of neutrons with the energy $E_n = 265$ neV above the asymmetric barrier for two durations of the incident pulse (the structure parameters are given in Fig. 4). For the pulse duration $\tau_0 = 660$ ns and the energy spectrum width $\Delta E = 1$ neV, the peak of the reflected pulse indeed shifts to the left by $\Delta t = -316$ ns (Fig. 6b, curve *2*). This corresponds to a negative real-valued group time of about half of the limit GDT value $\tau_m = -541$ ns obtained in the plane-wave approximation. If the incident pulse duration diminishes to $\tau_0 = 165$ ns (the spectrum width $\Delta E = 4$ neV), the shift of the maximum in the time distribution of the reflected pulse diminishes to $\Delta t = -74$ ns (Fig. 6c, curve *2*). An increase in the spectrum width by a factor of four corresponds in this case to a larger width of the function $A_0(\Omega)$ in the background of a dip in the reflection coefficient $r(\omega)$ in integral (48) and on curve *2* in Fig. 4a; as a result, the overall intensity of the reflected pulse also increases by approximately a factor of four. We also note that the reflected pulse now has a double-peak shape.

Figure 6 shows that the definition of a negative GDT is to some extent formal. The peak of the reflected packet actually comes somewhat earlier than the peak of the incident wave package, but there is no contradiction whatsoever between this phenomenon and the causality principle. The negative time is a consequence of different shapes of the incident and reflected pulses, which occurs because in addition to reflecting waves, the structure also transmits them, and this phenomenon is strongly energy dependent.

Similar results have also been obtained for an asymmetric three-layer structure (Fig. 7) (the structure parameters are given in the caption to Fig. 5). Figure 7a shows the relation between the shape and positions of the incident and reflected pulses for incident waves coming from the side of a narrower barrier. The energy spectrum of the transmission through the three-layer structure has the maximum at the energy $E_n \approx 144$ neV (see Fig. 5). For a wave packet whose duration is $\tau_0 = 165$ ns, the spectrum width is $\Delta E = 4$ neV, and the maximum is located at 144 neV, the delay time of the maximum proved to be $\Delta t = 227$ ns, a value that is approximately 1.5 times smaller than the GDT value $\tau_m = 377$ ns calculated using Eqn (10) in the plane-wave approximation. An even more significant difference between the results obtained for plane waves and a wave packet is observed if the pulse comes from the side of a broader barrier (Figs 7b, c) when the GDT is negative. For a pulse with the energy width of 4 neV, this time is $\Delta t = -21$ ns (Fig. 7b, curve *2*). If the packet width is reduced to 1 neV, the negative packet delay time $\Delta t = -66$ ns (Fig. 7c) differs less from the ideal value $\tau_m = -80$ ns.

In this case as well, the negative value of the delay time does not contradict the causality principle. The packet shift is due to changes in its magnitude and shape, because part of the flux is transmitted through the potential structure.

There is another method equivalent to the spectral approach described above, which is based on decomposing the wave function into plane waves. This method uses the concept of a response function in the direct space t. The amplitude of the reflected wave can be represented in an

integral form

$$A_{\mathrm{R}}(t) = \int_{-\infty}^{t} G(t-t')A_0(t')\,\mathrm{d}t'\,, \tag{56}$$

which explicitly takes the causality principle into account: $t' \leqslant t$. Here, $G(\tau)$ is the response function, also referred to as the point-like source (or Green's) function because, for the delta-shaped wave packet $A_0(t) = \delta(t-t_0)$, the reflected signal is $A_{\mathrm{R}}(t) = G(t-t_0)$. By comparing (56) and (48), we can readily derive a relation between the response function and the amplitude reflection coefficient:

$$G(\tau) = \frac{1}{2\pi}\int_{-\infty}^{\infty} r(\omega_0+\Omega)\exp(-\mathrm{i}\Omega\tau)\,\mathrm{d}\Omega\,. \tag{57}$$

Formulas similar to Eqns (56) and (57), where the time t is replaced with the coordinate x and the frequency detuning Ω with the difference in the x projections of the wave vectors $q = k_x - k_{0x}$, are also valid for the bounded monochromatic beam considered in Section 4.1.

5. Prospects of experimental observation

5.1 Direct measurement of the Goos–Hänchen shift

We have shown in Section 4 that at resonance, the time τ of the delay from multilayer structures can have a positive or negative value of the order of 100–500 ns. This observation has been confirmed experimentally. The point is that if thermal or cold neutrons are incident on a resonance structure at a glancing angle, the beam shift in the waveguide region $\xi = V_x\tau$ attains macroscopic levels. Therefore, the neutrons that entered the wave-guiding layer at distances smaller than ξ from the farther end of the sample can leave it not by tunneling through external layers but directly via the butt end of the sample. Such radiation was recorded in experiments [80–82]. GH-type experiments usually measure the reflected beam shift rather than the longitudinal shift $\xi = V_x\tau$, the former being proportional to the latter and having the value $d = (V_z/V_0)\xi$ in the transverse direction (see Fig. 1). Substituting formula (11) for ξ and the formula for the total velocity V_0 in the last relation, we obtain

$$d = \frac{V_x V_z}{\sqrt{V_x^2+V_z^2}}\,\tau \approx V_z\tau\,, \qquad V_z \ll V_x\,. \tag{58}$$

Because total (or almost total) reflection is usually considered, the neutron velocity V_z normal to the medium surface is of the order of several meters per second. For this reason, the inequality in (58) holds well for all neutrons except the slowest (ultracold) ones. The transverse shift then depends on the normal velocity V_z alone. Under the conditions of TER from a homogeneous medium, the beam shift is $d \approx V_z\tau \approx 10-50$ nm, a value that can hardly be measured.

Applying multilayer structures allows using a resonant enhancement of the GDT and the beam shift proportional to it. The value of the transverse shift can be as large as 1 μm, and hence the corresponding experiments are feasible. The resonant behavior of the effect enables resolving another significant problem. The shift is small everywhere except a narrow resonance region, and the position of the beam outside the resonance can be taken as a reference from which the relatively large resonance shift is to be measured.

It is natural to assume that the experiment can be carried out using a reflectometer operating in the time-of-flight mode [57]. In this configuration, a narrow neutron beam is incident on the sample at a fixed glancing angle θ, and the normal component of the wave vector $k_z(t) = k_0(t)\sin\theta$ depends on the time of flight. Thus, the reflected beam shifts from the reference position in only a narrow and well-known range of time-of-flight values.

5.2 Measuring the group delay time

Direct and correct measurement of the GDT for reflected neutron pulses does not seem to be feasible. A direct experiment is possible in optics owing to the availability of a femtosecond light source [83, 84], while sufficiently short neutron pulses cannot be produced.

The feasibility of the experiment can be discussed based on the observation of the interference of the reference wave with a wave packet delayed by a time Δt as a result of interaction with a resonant structure. As a result, it is shifted along the direction of propagation by a $\Delta x = (\hbar k/m)\Delta t$, which corresponds to the phase change $\Delta\varphi = k\Delta x$ (here, k is the total wavenumber, which is quite close to k_x, however). Such an experiment is feasible in principle using an interferometer that is intended for long-wave, so-called cold, neutrons [85–87]. However, the correctness of the experiment is based on an assumption that is far from obvious: that the spectral composition of the packet does not change as a result of interaction.

The same assumption underlies another method for measuring the interaction time, named the Larmor clock. This method originates from Baz's proposal [88] to use that clock as a theoretical technique for calculating the time during which a particle interacts with a 3D potential. Baz's idea is briefly as follows.

We assume that in a sphere of radius R containing a region where the potential is effective, there is an infinitely small magnetic field B directed along the z axis. If a spin-1/2 particle directed along the x axis enters this sphere, its spin starts rotating with the Larmor frequency $\omega_{\mathrm{L}} = 2\mu B/\hbar$. Due to this, the spin of the particle that was scattered and left the sphere is rotated by an angle θ. This angle can be calculated to yield the average time $\Delta t_{\mathrm{L}}(E) = \theta/\omega_{\mathrm{L}}$ during which the particle stayed in the magnetic-field region. It is apparent that to determine the proper interaction time τ in this way, the time Δt_{L} must be diminished by the time needed for the particle to fly through a sphere of radius R in the absence of the potential.

It can easily be shown that the Larmor time Δt_{L} determined in this way is closely related to the GDT [89]. Indeed, the Larmor precession angle θ can be identified with the phase difference $\Delta\varphi$ of the two wave functions that correspond to two spin projection values on the z axis and differ by the wavenumber values:

$$k_{\pm} = k_0\left(1 \pm \frac{\mu B}{E}\right)^{1/2}, \qquad E = \frac{\hbar^2 k_0^2}{2m}\,, \tag{59}$$

where k_0 is the wavenumber of the neutron in the absence of a field, μ is the magnetic moment, and B is the magnetic induction. Having determined the time $\Delta t_{\mathrm{L}}(E) = \Delta\varphi/\omega_{\mathrm{L}}$ following [88] and taking into account that $2\mu B = \Delta E$, we obtain the relation $\Delta t_{\mathrm{L}} = \hbar(\Delta\varphi/\Delta E)$, which coincides in the limit $B \to 0$ with Eqns (10) and (52).

We note that this conclusion does not involve the nonobvious assumption that the precession frequency ω_{L} remains constant in the process of interaction: in considering

the problem of a nonadiabatic entry of a particle into a magnetic field region, we can only use such terms as the difference in wavenumbers $k_\pm$ and the phase difference $\Delta\varphi(z) = (k_+ - k_-)z$. In the case of free translational motion of a particle in a magnetic field region, the precession angle can be expressed in terms of the Larmor frequency $\theta(L) = \omega_L(L/V)$, where the distance L is measured from the region boundary. Thus, the precession angle depends only on the coordinate and not on time, and the concept of frequency does not reflect the physical nature of the phenomenon.

If a particle interacts with a potential, any attempt to trace its coordinate is absolutely incorrect. Thus, the statement repeatedly made in publications that the Larmor clock method is based on using the Larmor frequency as a universal time standard is not quite true, although this circumstance does not cast doubt on the conclusion about the relation between the Larmor time and the group time introduced by Bohm and Wigner. The difficulty described above can easily be removed if we instead compare the precession angles of the particles that passed through a magnetic field region with and without a potential.

Baz's idea [88] proved to be very fruitful, at least if used as a theoretical technique. Rybachenko [90] applied that idea to calculate the time during which a particle tunnels through a potential barrier.

The concept of Larmor time is present in many theoretical studies that focus primarily on the tunneling time problem (see, e.g., reviews [91, 92]). It was shown at the same time that the method is not free from some intrinsic problems. One of them is the necessity to take the emergence of polarization along the z axis into account [93], which is due to the energy dependence of the transmission and reflection amplitudes of the object under study, reflection and interference of waves on the interface between the regions with and without a potential, and a number of other reasons.

The Larmor clock method has been used in neutron optics to measure the delay time caused by refraction, reflection from a multilayer structure, and tunneling in a quasi-bound-state resonance [89, 94–96]. Experiments used a spin-echo spectrometer [97, 98] that contained two solenoids tuned such that if the neutron velocity did not change, the large spin precession angle that occurred when the neutron passed through a solenoid was fully compensated in passing through the other solenoid. The sample under study was placed into a solenoid such that the total precession angle was determined by the phase difference of the two spin components that emerged as a result of the interaction with the sample. The precession phase in the beam that passed through the sample was compared with that of the reference beam. Possible transformation of the spectrum as a result of interaction with the object was ignored. Although the results obtained have a semi-quantitative character, they satisfactorily agree with theoretical estimates. The sensitivity of time measurement was about 0.5 ns, almost an order of magnitude smaller than the GDT in TER.

Given the limitations described above, this method also seems to be applicable to measuring the positive and negative time of reflection from multilayer structures.

6. Conclusions

The well-known GH effect was discussed in this paper from the standpoint of the reflection of neutrons from matter. The longitudinal shift of the reflected beam was shown to be determined in all cases by the product of the longitudinal velocity of the neutron and the GDT. If neutrons exhibit TER, this shift is rather small and can hardly be detected. But in the case of reflection from planar multilayer structures, the shift effect can be enhanced in a resonant way, and, under certain conditions, the GDT and longitudinal shift can be negative. We stress that the equations that determine the GDT follow from an approximate analysis, and the concept of the GDT per se is nothing but an estimate of the reflection time.

A more correct analysis of the wave packet transformation for reflection from a resonant structure allows concluding that the negative time shift is due to a change in the time pulse shape and does not contradict the causality principle.

This conclusion, however, does not compromise the feasibility of both the experimental observation of positive and negative shifts of neutron beams under reflection and the direct measurement of the reflection time. The use of resonant structures in both cases offers new experimental approaches. It was proposed to use a time-of-flight neutron reflectometer to measure the GH shift. As regards the direct measurement of the neutron reflection time, the conceptual possibility to measure the GDT of the reflected beam has already been demonstrated in neutron experiments with the Larmor clock.

References

1. Goos F, Lindberg-Hänåhen H *Ann. Physik* **436** 333 (1947)
2. Goos F, Lindberg-Hänchen H *Ann. Physik* **440** 251 (1949)
3. Artmann K *Ann. Physik* **437** 87 (1948)
4. Fragstein C V *Ann. Physik* **439** 271 (1949)
5. Brekhovskikh L M *Usp. Fiz. Nauk* **50** 539 (1953)
6. Renard R H *J. Opt. Soc. Am.* **54** 1190 (1964)
7. Lotsch H K V *J. Opt. Soc. Am.* **58** 551 (1968)
8. Tamir T, Oliner A A *J. Opt. Soc. Am.* **59** 942 (1969)
9. Lotsch H K V *Optik* **32** 116 (1970)
10. Horowitz B R, Tamir T *J. Opt. Soc. Am.* **61** 586 (1971)
11. McGuirk M, Carniglia C K *J. Opt. Soc. Am.* **67** 103 (1977)
12. Snyder A W, Love J D *Appl. Opt.* **15** 236 (1976)
13. Carniglia C K *J. Opt. Soc. Am.* **66** 1425 (1976)
14. Fedorov F I *Zh. Priklad. Spektrosk.* **27** 580 (1977)
15. Yasumoto K, Oishi Y *J. Appl. Phys.* **54** 2170 (1983)
16. Lai H M, Cheng F C, Tang W K *J. Opt. Soc. Am. A* **3** 550 (1986)
17. Fedoseyev V G *J. Opt. Soc. Am. A* **3** 826 (1986)
18. Puri A, Birman J L *J. Opt. Soc. Am. A* **3** 543 (1986)
19. Ghatak A K et al. *Opt. Commun.* **56** 313 (1986)
20. Shi J-L, Li C-F, Wang Q *Int. J. Mod. Phys. B* **21** 2777 (2007)
21. Rhodes D J, Carniglia C K *J. Opt. Soc. Am.* **67** 679 (1977)
22. Bretenaker F, Le Floch A, Dutriaux L *Phys. Rev. Lett.* **68** 931 (1992)
23. Pfleghaar E, Marseille A, Weis A *Phys. Rev. Lett.* **70** 2281 (1993)
24. Gilles H, Girard S, Hamel J *Opt. Lett.* **27** 1421 (2002)
25. Merano M et al. *Opt. Express* **15** 15928 (2007)
26. Schwefel H G L et al. *Opt. Lett.* **33** 794 (2008)
27. Moskalenko V V, Soboleva I V, Fedyanin A A *JETP Lett.* **91** 382 (2010); *Pis'ma Zh. Eksp. Teor. Fiz.* **91** 414 (2010)
28. Schoch A *Ergeb. Exakten. Naturwiss.* **23** 127 (1950)
29. Schoch A *Acustica* **2** 1 (1952)
30. Schoch A *Acustica* **2** 18 (1952)
31. Declercq N F, Degrieck J, Leroy O *Appl. Phys. Lett.* **85** 4234 (2004)
32. Akylas V, Kaur J, Knasel T M *Appl. Opt.* **13** 742 (1974)
33. Arthur L et al. *J. Opt. Soc. Am.* **68** 319 (1978)
34. Riesz R P, Simon R *J. Opt. Soc. Am. A* **2** 1809 (1985)
35. Haibel A, Nimtz G, Stahlhofen A A *Phys. Rev. E* **63** 047601 (2001)
36. Müller D et al. *Europhys. Lett.* **73** 526 (2006)
37. Tamasaku K, Ishikawa T *Acta Cryst. A* **58** 408 (2002)
38. Fedorov F I, in *Intern. Conf.* "*Spins and Photonic Beams at Interface*", *SPBI'2011, in the Framework of Fedorov Memorial Symp. Book of Abstracts and Programme, September 25–26, 2011, Minsk, Belarus* (Ed. S Ya Kilin) (Minsk: Stepanov Institute of Physics, 2011) p. 8; http://master.basnet.by/congress2011/sympo-

sium/spbi.pdf; Translated from Russian: *Dokl. Akad. Nauk SSSR* **105** 465 (1955)
39. Imbert C *Phys. Rev. D* **5** 787 (1972)
40. Pillon F, Gilles H, Girard S *Appl. Opt.* **43** 1863 (2004)
41. Cowan J J, Aničin B *J. Opt. Soc. Am.* **67** 1307 (1977)
42. Li C-F *Phys. Rev. A* **76** 013811 (2007)
43. Dennis M R, Götte J B *New J. Phys.* **14** 073013 (2012)
44. Aiello A, Woerdman J P *Opt. Lett.* **33** 1437 (2008)
45. Aiello A *New J. Phys.* **14** 013058 (2012)
46. Carniglia C K, Brownstein K R *J. Opt. Soc. Am.* **67** 121 (1977)
47. Lai H M, Chan S W, Wong W H *J. Opt. Soc. Am. A* **23** 3208 (2006)
48. Hora H *Optik* **17** 409 (1960)
49. Carter J L, Hora H *J. Opt. Soc. Am.* **61** 1640 (1971)
50. Agudin J L *Phys. Rev.* **171** 1385 (1968)
51. Seregin A A *Sov. J. Nucl. Phys.* **33** 622 (1981); *Yad. Fiz.* **33** 1173 (1981)
52. Mâaza M, Pardo B *Opt. Commun.* **142** 84 (1997)
53. Ignatovich V K *Phys. Lett. A* **322** 36 (2004)
54. de Haan V-O et al. *Phys. Rev. Lett.* **104** 010401 (2010)
55. Ignatovich V K *Phys. Rev. Lett.* **105** 018901 (2010)
56. de Haan V-O et al. *Phys. Rev. Lett.* **105** 018902 (2010)
57. Frank A I *J. Phys. Conf. Ser.* **528** 012029 (2014)
58. Eisenbud L, Ph.D. Thesis (Princeton: Princeton Univ., 1948)
59. Bohm D *Quantum Theory* (New York: Prentice-Hall, 1951) p. 257; Translated into Russian: *Kvantovaya Teoriya* (Moscow: Nauka, 1965) p. 305
60. Wigner E P *Phys. Rev.* **98** 145 (1955)
61. Tamir T, Bertoni H L *J. Opt. Soc. Am.* **61** 1397 (1971)
62. Levy Y, Imbert C *Opt. Commun.* **13** 43 (1975)
63. Schreier F, Schmitz M, Bryngdahl O *Opt. Lett.* **23** 576 (1998)
64. Felbacq D, Moreau A, Smaâli R *Opt. Lett.* **28** 1633 (2003)
65. de Beauregard O C, Imbert C, Levy Y *Phys. Rev. D* **15** 3553 (1977)
66. Chen L et al. *Opt. Lett.* **32** 1432 (2007)
67. Aničin B A, Fazlić R, Koprić M *J. Phys. A* **11** 1657 (1978)
68. Wild W J, Giles C L *Phys. Rev. A* **25** 2099 (1982)
69. Declercq N F et al. *Appl. Phys. Lett.* **82** 2533 (2003)
70. Li C-F, Wang Q *Phys. Rev. E* **69** 055601(R) (2004)
71. Liu X et al. *Phys. Rev. E* **73** 056617 (2006)
72. Breazeale M A, Torbett M A *Appl. Phys. Lett.* **29** 456 (1976)
73. Bonnet C et al. *Opt. Lett.* **26** 666 (2001)
74. Yin X et al. *Appl. Phys. Lett.* **85** 372 (2004)
75. Vetter R-M, Haibel A, Nimtz G *Phys. Rev. E* **63** 046701 (2001)
76. Chen X, Li C-F *Eur. Phys. J. B* **46** 433 (2005)
77. Xiao Z, Du S, Zhang C-X, arXiv:1210.0970
78. Olkhovsky V S, Recami E, Zaichenko A K *Europhys. Lett.* **70** 712 (2005)
79. Vinogradova M B, Rudenko O V, Sukhorukov A P *Teoriya Voln* (Wave Theory) (Moscow: Fizmatlit, 1990)
80. Pfeiffer F et al. *Phys. Rev. Lett.* **88** 055507 (2002)
81. Kozhevnikov S V et al. *JETP* **117** 636 (2013); *Zh. Eksp. Teor. Fiz.* **144** 733 (2013)
82. Kozhevnikov S V et al. *JETP* **123** 950 (2016); *Zh. Eksp. Teor. Fiz.* **150** 1094 (2016)
83. Chauvat D et al. *Phys. Rev. Lett.* **84** 71 (2000)
84. Chauvat D et al. *Phys. Lett. A* **336** 271 (2005)
85. Gruber M et al. *Phys. Lett. A* **140** 363 (1989)
86. Schellhorn U et al. *Physica B* **234–236** 1068 (1997)
87. Pruner C et al. *Nucl. Instrum. Meth. Phys. Res. A* **560** 598 (2006)
88. Baz' A I *Sov. J. Nucl. Phys.* **4** 182 (1967); *Yad. Fiz.* **4** 252 (1966)
89. Frank A I et al. *Physica B* **297** 307 (2001)
90. Rybachenko V F *Sov. J. Nucl. Phys.* **5** 484 (1967); *Yad. Fiz.* **5** 895 (1967)
91. Hauge E H, Støvneng J A *Rev. Mod. Phys.* **61** 917 (1989)
92. Olkhovsky V S, Recami E, Jakiel J *Phys. Rep.* **398** 133 (2004)
93. Büttiker M *Phys. Rev. B* **27** 6178 (1983)
94. Frank A I et al. *JETP Lett.* **75** 605 (2002); *Pis'ma Zh. Eksp. Teor. Fiz.* **75** 729 (2002)
95. Frank A I et al. *Phys. At. Nucl.* **65** 2009 (2002); *Yad. Fiz.* **65** 2066 (2002)
96. Frank A I et al. *Lecture Notes Phys.* **601** 165 (2002)
97. Mezei F *Lecture Notes Phys.* **601** 5 (2002)
98. Schleger P et al. *Physica B* **241–243** 164 (1997)